THE JOURNAL OF PHYSICAL CHEMISTRY LETTERS
A JOURNAL OF THE AMERICAN CHEMICAL SOCIETY

pubs.acs.org/JPCL

Letter

Transferability and Accuracy of Ionic Liquid Simulations with Equivariant Machine Learning Interatomic Potentials

Zachary A. H. Goodwin,* Malia B. Wenny, Julia H. Yang, Andrea Cepellotti, Jingxuan Ding, Kyle Bystrom, Blake R. Duschatko, Anders Johansson, Lixin Sun, Simon Batzner, Albert Musaelian, Jarad A. Mason, Boris Kozinsky,* and Nicola Molinari*

Cite This: *J. Phys. Chem. Lett.* 2024, 15, 7539−7547

Read Online

ACCESS | Metrics & More | Article Recommendations | Supporting Information

ABSTRACT: Ionic liquids (ILs) are an exciting class of electrolytes finding applications in many areas from energy storage to solvents, where they have been touted as "designer solvents" as they can be mixed to precisely tailor the physiochemical properties. As using machine learning interatomic potentials (MLIPs) to simulate ILs is still relatively unexplored, several questions need to be answered to see if MLIPs can be transformative for ILs. Since ILs are often not pure, but are either mixed together or contain additives, we first demonstrate that a MLIP can be trained to be compositionally transferable; i.e., the MLIP can be applied to mixtures of ions not directly trained on, while only being trained on a few mixtures of the same ions. We also investigated the accuracy of MLIPs for a novel IL, which we experimentally synthesize and characterize. Our MLIP trained on ∼200 DFT frames is in reasonable agreement with our experiments and DFT.

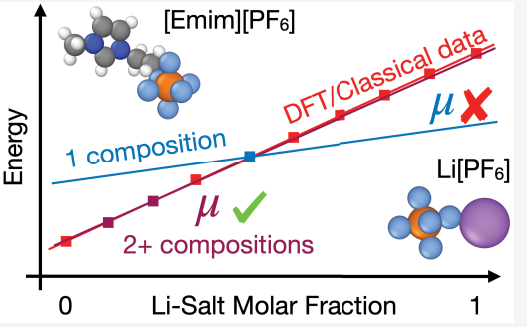

Ionic liquids (ILs) are a unique and highly promising class of electrolytes that contain no solvent in their neat form.[1−3] This lack of solvent, such as organic carbonates or water, makes ILs advantageous for numerous applications from supercapacitors/batteries,[4−6] to gas storage,[7,8] to themselves acting as "green solvents" for chemical reactions.[1,3] These applications benefit from the use of ILs because ILs have extremely low vapor pressure, are nonflammable, and can withstand large voltages without decomposing,[1−4] which are a set of properties that water and organic carbonates do not possess. The unique properties of ILs come, in part, from the large, highly asymmetric and ionic nature of the molecular species which comprise the IL.[1−4] Moreover, ILs can be mixed to tune desired physiochemical properties, creating a class of "designer solvents" with a huge chemical space.[9]

As ILs are often composed of large, complicated, molecular ions, this has meant atomistic simulations are necessary for quantitative predictions of these concentrated electrolytes.[4,6,10−12] Typically, classical molecular dynamics (MD) has been used to simulate ILs and calculate physiochemical properties,[4,6,12,13] largely because 1,000+ atoms can routinely be simulated for 1+ ns, which are the length and time scales typically required for ILs. The accuracy of the predictions from classical force fields is often under question, however,[14] which motivates some to use *ab initio* MD (AIMD) to simulate ILs.[6] However, running density functional theory (DFT) is prohibitively expensive in comparison, which limits the simulations to short time scales (∼100 ps) and system sizes (∼100s of atoms).[6]

Machine learning interatomic potentials (MLIPs) have promised a way to bridge this efficiency−accuracy gap in atomistic simulations.[6,15−19] In the context of ILs, there have been several works which develop MLIPs for specific electrolytes, such as the work of Montes-Campos et al.,[20] Dajnowics et al.,[14] and Ling et al.[21] for room temperature ILs and the work of Tovey et al.,[22] Li et al.,[23] Mondal et al.,[24] and Liang et al.[25] for molten salts. These works often employ large data sets, e.g., with 1,000+ DFT calculations, mainly focus on the NVT ensemble, and typically only developed a model for one neat IL or molten salt. With the recent development of equivariant MLIPs, such as NequIP/Allegro[26−28] and MACE,[29] training a MLIP for a specific application has become significantly more accurate and data efficient. Hence, using equivariant MLIPs[26−29] to simulate ILs should provide an unprecedented accuracy/efficiency trade-off, but there are questions which remain to be answered if these MLIPs are to transform IL simulations and bridge this gap.

Received: July 2, 2024
Revised: July 12, 2024
Accepted: July 12, 2024
Published: July 18, 2024

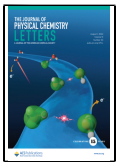

https://doi.org/10.1021/acs.jpclett.4c01942
J. Phys. Chem. Lett. 2024, 15, 7539−7547

In this work, we aim to answer how to train a compositionally transferable MLIP and establish the accuracy of a MLIP for a novel IL with relatively little training data. To test the compositional transferability, we choose to study a common salt-in-IL, $Li^+[PF_6]^-$ in $[EMIM]^+[PF_6]^-$, which has recently attracted attention because the Li^+ has been observed to have a negative transference number at low salt molar fractions, as has been well studied from classical MD[30−33] and experiments.[34,35] We demonstrate that NequIP/Allegro can learn to be transferable, i.e., having a model with similar accuracy for compositions not trained on as those that were trained on, while only being trained on several compositions, *but only if these compositions are carefully chosen*. Of the routes tested, we find that at least 2 compositions are required, and the best approach is to train on "high-entropy" Li-salt molar fractions, e.g., 0.4−0.6, as these compositions ensure interactions are well sampled. Second, we synthesize and experimentally characterize a novel IL, $[F\text{-}OMIM]^+[C_4F_9CO_2]^-$, which is similar to other ILs of interest for their high O_2 solubility.[8,36] We investigate how to train an accurate Allegro model with ∼200 DFT frames, capable of capturing experimental densities, thermal expansion, and isothermal compressibility of this novel $[F\text{-}OMIM]^+[C_4F_9CO_2]^-$, with the main limitation being the approximations of our chosen DFT settings. For $[F\text{-}OMIM]^+[C_4F_9CO_2]^-$ we also investigate the role of how the structures are generated and perform a hyperparameter search to optimize the model.

In the Supporting Information, we provide the experimental details for the synthesis and characterization of $[F\text{-}OMIM]^+[C_4F_9CO_2]^-$ (Section 1)[8,36] and additional details for the computational methods employed that are briefly described below (Sections 2−5).

We use classical MD simulations to generate a diverse set of uncorrelated structures of the two ILs studied here, $[F\text{-}OMIM]^+[C_4F_9CO_2]^-$ and $Li^+[PF_6]^-$ in $[EMIM]^+[PF_6]^-$. Since the MD simulations for these two ILs are almost identical, we describe our method and point out any differences between them. The procedure to generate the initial, equilibrated structures is outlined in the Supporting Information Section 1.[30,30,31,37−39]

The classical MD simulations have periodic boundary conditions, use a time step of δt = 1.0 fs, a velocity-Verlet algorithm to evolve the equations of motion, a Nosé−Hoover barostat (1000 δt coupling) and thermostat (100 δt coupling) to enforce pressure and temperature, respectively,[40−42] and are performed using the LAMMPS code.[43,44] The atomic interactions are modeled with OPLS-AA[45] with parameters obtained from ref 46. For $Li^+[PF_6]^-$ in $[EMIM]^+[PF_6]^-$, to reproduce realistic densities, we rescale the atomic charges to 80% of the original value.[30,46−48] Whereas, for $[F\text{-}OMIM]^+[C_4F_9CO_2]^-$ we rescale the atomic charges by 70% to match our experimental data better (see Supporting Information Section 4).

For $Li^+[PF_6]^-$ in $[EMIM]^+[PF_6]^-$ we investigate Li-salt molar fractions ranging from 0.0 to 1.0, in increments of 0.1, with 20 ion pairs in the simulation box for each composition. For each composition, two initial structures were generated: one for training and validation and another for testing the trained models. To generate these data sets, each structure is evolved for 80 ns in the NVT ensemble at 300 K. The atomic positions and force components are saved every 20 ps to generate a total of 4000 snapshots for each composition.

For $[F\text{-}OMIM]^+[C_4F_9CO_2]^-$, we simulate three different temperatures (300, 450, and 600 K) in the NPT ensemble with a pressure of 1 atm, with 10 ion pairs in the simulation box. For every new temperature, we first let the system equilibrate for 1 ns and then run for 6 ns, during which snapshots of the structure are saved every 20 ps to ensure sufficient decorrelation. Thus, we generated a total of 900 snapshots, 300 per temperature.

To obtain accurate energy, force, and stress data, we performed density functional theory (DFT) calculations using Quantum Espresso.[49,50] We utilize the PBE exchange-correlation functional,[51] D3[52] dispersion correction for van der Waals interactions, and use the ultrasoft pseudopotentials from ref 53. We use Γ-point sampling, a cutoff of 50 Ry for the wave functions, a cutoff of 500 Ry for the charge density, and a convergence threshold of 10^{-10} Ry.

For $Li^+[PF_6]^-$ in $[EMIM]^+[PF_6]^-$, we performed DFT calculations on 50 frames (equally spaced to maximize decorrelation) from each composition and run. For $[F\text{-}OMIM]^+[C_4F_9CO_2]^-$, we initially selected 60 frames (again, equally spaced) at each temperature to generate a small DFT training data set. Starting from these structures, we also performed fixed-cell AIMD on each structure for 50 steps (with a ∼1 fs time step) at the corresponding temperatures (using the Verlet algorithm and a tolerance for rescaling velocities of 10 K) and also 10 steps of fixed-cell relaxation for each structure. We also calculated the single atom energies of all the elements in these frames, from only keeping each element in a box with a length of ∼30 Å.

We use the state-of-the-art graph neural network MLIPs, NequIP[26] and Allegro,[27,28] to train, validate, and run the simulations for these ILs. Initially, NequIP was used to perform the transferability test on the SiIL. NequIP is an equivariant message-passing graph neural network with unprecedented accuracy, but because of its message-passing architecture, it cannot be scaled to large systems efficiently. Allegro is a simplification of NequIP, without the message passing architecture because of the local cutoff, that can be scaled to large systems efficiently. Therefore, we also performed a transferability test with Allegro and only used Allegro to run simulations in LAMMPS. We refer the readers to refs 26−28 for an extensive explanation of the network architecture and the importance of equivariant models.[19]

For the classical data set of $Li^+[PF_6]^-$ in $[EMIM]^+[PF_6]^-$, to perform the initial transferability test with NequIP, we use r_{max} = 5, l_{max} = 1 with irreps 16x0o + 16x0e + 8x1o + 8x1e, with 5 layers, and use a learning rate of 0.05 with a batch size of 5. For each composition we use 650 frames (equally spaced)—600 frames for training and 50 frames for validation—and when multiple compositions are trained on these data sets are combined, increasing the total number of frames trained on. The test set was an independent set of 650 frames for each composition. While clearly the models will not possess a greater accuracy than that of the classical force field; here we do not aim for accurate models, but rather aim to understand the intricacies of training a transferable model for ILs.

To perform the transferability tests with Allegro, we choose r_{max} = 6, l_{max} = 2, n_{layers} = 2, learning rate of 0.0005, batch size of 1, and 80−20% split of training validation data and find that it is essential to employ single atom energies when training on multiple compositions with DFT data from Quantum Espresso. Only 50 frames (equally spaced) from each of the

https://doi.org/10.1021/acs.jpclett.4c01942
J. Phys. Chem. Lett. 2024, 15, 7539−7547

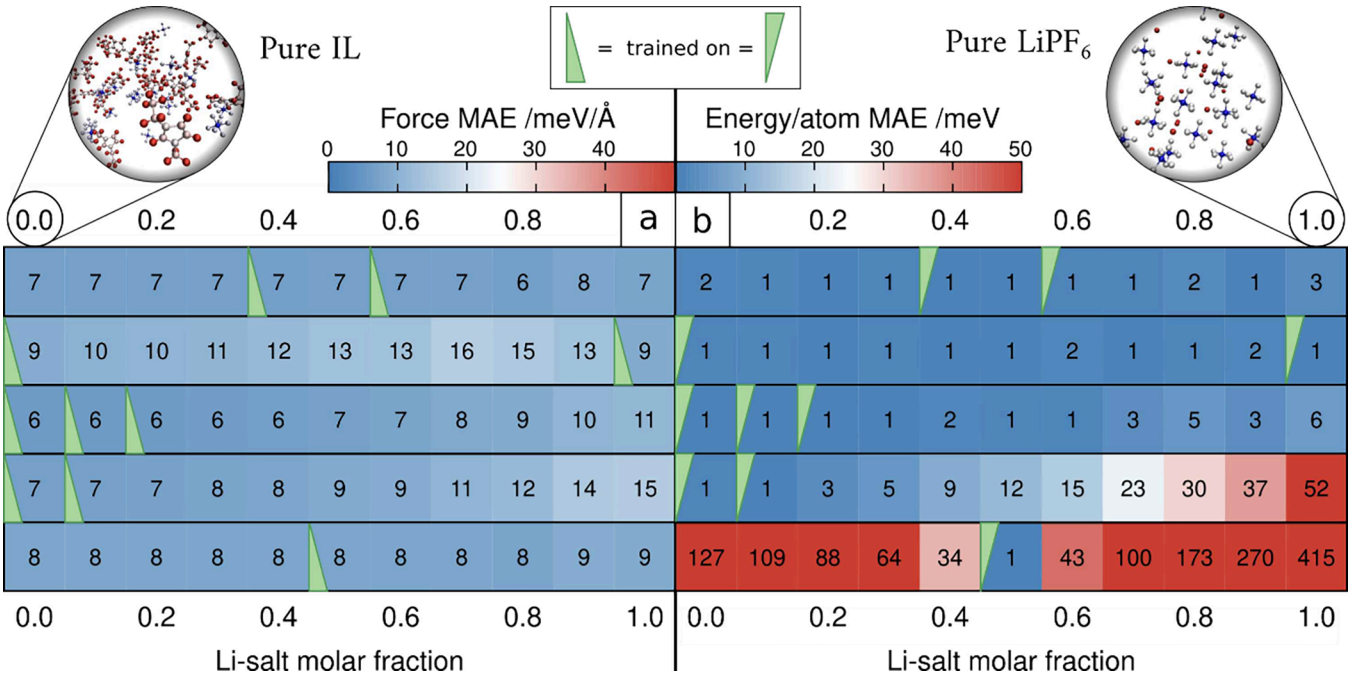

Figure 1. Transferability investigation of NequIP for a typical salt-in-IL, $Li^+[PF_6]^-$ in $[EMIM]^+[PF_6]^-$, trained on classical data. Each row corresponds to a different NequIP model trained on the molar fractions shown by the green triangles. Each number at each molar fraction is the mean absolute error (MAE) on an independent test set for forces, as shown on the left (a) in units of meV/Å and energy on the right (b) in units of meV/atom.

training/validation and test sets were selected to form the DFT calculations for the test.

Note that this transferability investigation using test errors allows us to identify only which models are certainly failing from large errors. As good errors do not provide a conclusive measure of if a MLIP is stable and reliable when being run, further testing will be needed if these models are to be used to calculate physiochemical properties (see Supporting Information Section 5 for the protocol of $[F\text{-}OMIM]^+[C_4F_9CO_2]^-$).

The results shown for $[F\text{-}OMIM]^+[C_4F_9CO_2]^-$ in the main text are based on a single Allegro model (see Supporting Information Section 5). We choose $r_{max} = 7$, $l_{max} = 2$, $n_{layers} = 2$, LR = 0.001, batch size of 4, stress weight of 100 (with force and energy of 1), and 80−20% split of training validation data.

To run these models, we employed LAMMPS with a custom pair style. We use the Nosé−Hoover barostat (1000 δt coupling) and thermostat (100 δt coupling) to enforce pressure and temperature with a time step of $\delta t = 0.5$ fs. To obtain the isothermal compressibility, we first equilibrated the system at 1 bar for 50 ps. Then the pressure was increased by 1 kbar and equilibrated again for 50 ps before running for another 50 ps at this pressure for production; this process was repeated 18 times to obtain how the equilibrium volume changed with pressure, which was then fit to the Tait equation of state to obtain the isothermal compressibility.[8] Details of the other settings used for each calculation are presented in the results shown.

As outlined earlier, one of the most valuable properties of ILs is their ability to be mixed together to form "designer liquids" with physiochemical properties that can be precisely tuned.[9] Therefore, being able to simulate complex mixtures of ILs, and solutes, is a necessity. Typically, however, MLIPs are trained and tested on only a specific composition. This is because training older MLIP architectures built on invariant descriptors, such as GAP[18] and DeePMD,[54] require orders of magnitude more data, rendering them challenging enough to train for a single material. The recent advances in the accuracy and data efficiency of MLIPs, largely from equivariant architectures, have allowed the scope of these methods to expand.[19] One area that needs more quantitative attention is how to train a MLIP to be transferable and still be accurate enough to reliably use for calculations on compositions that it was not trained on. With the recent interest in "foundational" MLIPs,[55] this question is becoming even more important, and having quantitative, systematic tests of transferability on controlled data sets is valuable for these efforts.

With this question in mind, we chose to study the transferability of a well-known salt-in-IL (SiIL), $Li^+[PF_6]^-$ in $[EMIM]^+[PF_6]^-$, the results of which are shown in Figure 1. Each row represents a different NequIP model trained on classical data of specific molar fractions, as indicated by the green triangles, with the values at each molar fraction (in each box) being the test error on an independent data set. On the left is the force mean absolute error (MAE) in meV/Å, and the right is the energy MAE in meV/atom. In what follows, we describe the results and implications of Figure 1.

If a NequIP model is trained on a single composition at a Li-salt molar fraction of 0.5, we find the force MAE to be 8 meV/Å and the energy MAE to be 1 meV/atom at the same mole fraction. As we are using a large data set from a classical force field, these error values set the baseline, and we will not consider their values to be significant. For compositions away from the 0.5 molar fraction trained on the force, the MAE remains relatively constant, but the energy MAE increases to 100−400 meV/atom at the ends of the composition range. Therefore, training a NequIP model only on one composition works for the composition trained on, as is often done for MLIP, but the energy transferability of the NequIP model becomes worse the further out-of-distribution the composition becomes.

https://doi.org/10.1021/acs.jpclett.4c01942
J. Phys. Chem. Lett. 2024, 15, 7539−7547

Alternatively, multiple compositions could be trained on, which hopefully provides better transferability. The two rows above are examples of this strategy for adjacent compositions, trained on 2 and 3 compositions, comprising of the 0, 0.1 and 0, 0.1, 0.2 Li-salt molar fraction compositions, respectively. Again, the force MAEs are relatively constant across the entire composition range, albeit increasing to values larger than 10 meV Å^{-1} (approximately ×2 those trained on) at 0.9−1. The increase in force MAEs can be traced back to the increase in force errors of $Li^+[PF_6]^-$, with the forces of Li^+ becoming significantly worse. This is perhaps not surprising, as the interactions of $Li^+[PF_6]^-$ have not been sampled well. For the NequIP model trained on 2 compositions (0 and 0.1), the energy MAE increases to 30−50 meV/atom at 0.8−1 molar fraction, which is better than the model trained on a single composition but still corresponds to a ×50 increase. The model trained on 3 compositions (0−0.2) has similar trends, but the errors are slightly reduced in magnitude, and only corresponds to a ×6 increase in energy MAE at 1.0 Li-salt molar fraction.

Finally, if we train on 2 compositions, but not at one end of the composition range, we can obtain energy and force MAEs that are typically within ×2 of the MAEs of the compositions trained on. Training on the Li-salt molar fractions of 0 and 1 gives energy MAEs within ×2−3 over the entire composition range, and the force errors also remain within this limit. The increase in the force error for this model at intermediate Li-salt molar fractions can be traced back to an increase in the error of all elements, which could be rooted in the fact that no Li^+−$[EMIM]^+$ interactions are included in the data set. Overall, training on molar fractions of 0.4 and 0.6 results in a model with force and energy MAEs that are roughly constant across the entire composition range, i.e., within ×2 (apart from 1.0 Li-salt molar fraction compositions), which appears to be the best approach for training a transferable NequIP model for this system.

In Supporting Information Section 3, we show this same transferability test performed with Allegro, where we find qualitatively exactly the same results. To further ensure that these conclusions are robust, we performed a similar analysis where we took only 50 frames from the training/validation set and 50 frames from the test set and calculated the *ab initio* energies and forces to train an Allegro model (see Supporting Information Section 3). We find the conclusions drawn from the previous tests with classical force field data are robust, with the transferability investigation on only a small amount of DFT data to be qualitatively identical. *Therefore, such transferability tests can be performed with classical force field data first, before proceeding with expensive DFT calculations.* In addition, in Supporting Information Section 3 we show a transferability test for an example class of Li−P−S−Cl solid electrolyte and find the conclusions are again robust, further supporting our findings.

NequIP and Allegro learn directly on the force and energy values, with forces being atom-based quantities and the energy being the total energy of the simulation box. We find that the forces predicted by NequIP and Allegro generalize well, even if only 1 composition is sampled, but only provided interactions between species have been well sampled. This can be achieved from sampling from the middle of the composition range (0.4−0.6), or "high-entropy" configurations. Whereas, if we only sample from ends of the composition, the training data does not include enough cation−cation interactions, for example. The sampling of frames and compositions to learn forces more accurately could be achieved through employing uncertainty quantification,[56] as is typically used when performing active learning.[57,58]

In contrast, the generalization of the energy appears to be significantly more dependent on how many compositions are selected, which could be rooted in how MLIPs decompose the total energy into a sum of atomic energies, which is an uncontrolled approximation, at least in terms of the MLIP.[15,59,60] To understand these observations and generalize our results, we perform a simple analysis. Let us assume that there is just a single training frame for each composition. For the model trained on the Li-salt molar fraction of 0.5, let us assume the total energy can be written

$$E_{0.5} = \mu_{c1}N_{c1,0.5} + \mu_{c2}N_{c2,0.5} + \mu_a N_{a,0.5} \quad (1)$$

where μ_j and N_j are the energy per ion and the number of ions, respectively. Note that this simple, linear equation assumes no ions interact (i.e., the electrolyte is an ideal mixture), but this can still provide us insight into the energy generalization. The N_j values are known from the training data, but we are using the MLIP (we used NequIP/Allegro here, but the results are expected to apply to other methods[55]) to find the μ_j's. As we only have 1 equation but 3 unknowns, we are underdetermined, and no unique solution exits (as an infinite set of solutions are valid). Therefore, the MLIP solves for a linearly dependent set of values for μ_j which satisfy $E_{0.5}$, but the MLIP lacks constraints to reproduce E for other compositions. Thus, the energy generalizes poorly for this case (as clearly seen in Supporting Information Section 3).

Instead, for example, we train on the best case of Li-salt molar fractions of 0.4 + 0.6, and because $N_a = 20$ in all frames from the salts sharing the same anion, we can write the equations as

$$E_{0.4} - \mu_a N_a = \mu_{c1}N_{c1,0.4} + \mu_{c2}N_{c2,0.4} \quad (2)$$

and

$$E_{0.6} - \mu_a N_a = \mu_{c1}N_{c1,0.6} + \mu_{c2}N_{c2,0.6} \quad (3)$$

From these equations, we can determine μ_{c1} and μ_{c2} up to some arbitrary constant incorporated in μ_a. If fact, for this SiIL system, the only quantity which is well-defined is the energy difference between the cations, and it should not be possible to reliably determine all μ's without arbitrary constants. Therefore, with only 2 compositions to train on, the MLIP can learn how the energy should change with composition reasonably well. This logic explains why training on 2 compositions instead of 1 significantly helps, but training on 3 instead of 2 does not substantially improve learning the energy to be generalizable, as the third equation does not allow all the μ's to be determined uniquely.

If this is the case, we should find that the predictions of the energy of Li^+, for example, should not necessarily be the same across different models trained, but that the energy difference between Li^+ and $[EMIM]^+$ should be model independent (if trained on 2 or more compositions). We confirm with Allegro on DFT data that this is the case (at least approximately), as shown in Supporting Information Section 3.

Overall, it appears that the MLIPs struggle most with finding the linear, constant shift contributions to the energy from different species, but the methods can typically capture nonlinearities arising from local interactions. These observations allow us to generalize the results obtained here to have

https://doi.org/10.1021/acs.jpclett.4c01942
J. Phys. Chem. Lett. 2024, 15, 7539−7547

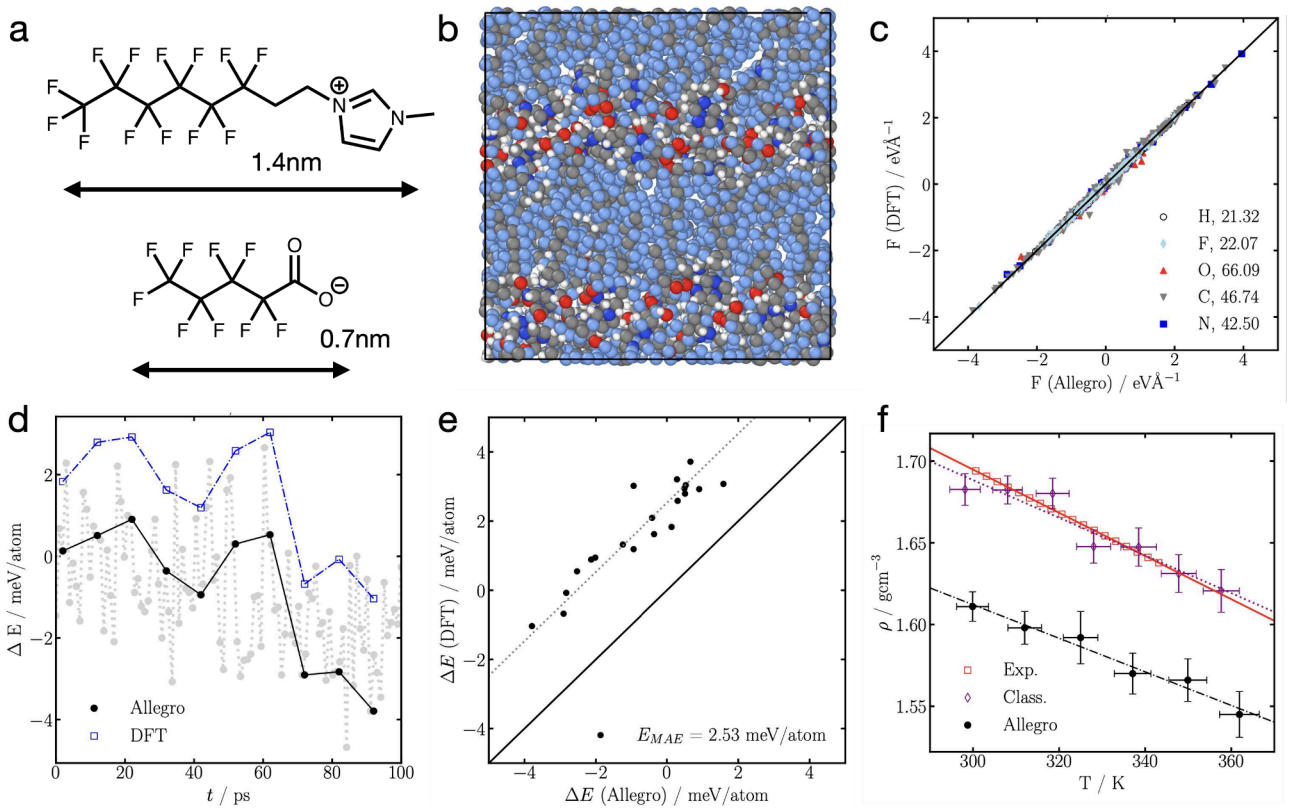

Figure 2. Allegro model for $[\text{F-OMIM}]^+[C_4F_9CO_2]^-$. (a) Schematic of $[\text{F-OMIM}]^+[C_4F_9CO_2]^-$, with approximate scale of each ion. (b) Structure of $[\text{F-OMIM}]^+[C_4F_9CO_2]^-$ showing its heterogeneous nature, generated using Ovito.[75] (c) Force parity plot between Allegro and DFT for all the elements and components from a single frame at 50 ps through an Allegro simulation at 300 K. Force MAE of each element is shown in the legend in units of meV Å^{-1} (d) Energy comparison between Allegro, and that calculated by DFT using the Allegro structure, as a function of time. The gray values are also Allegro but were not used to calculate energy/forces in DFT. (e) Energy parity plot between Allegro and DFT, half of the frames of which are shown in (d). (f) Comparison of density as a function of temperature for the experiments, classical force field, and the Allegro model (see the Supporting Information Section 5 for details).

some simple guidelines for training complex (ionic) mixtures. For an N-component, single phase, bulk system with M constraints (such as electroneutrality), we are required to sample $C = N - M$ unique compositions to ensure that the MLIP can learn how the total energy should (at least approximately) change with composition. Note that this condition sets the minimum number of compositions to sample to ensure the energy can be correctly learned, and using more compositions should mainly contribute improvements through there being more data, provided all interactions/environments have been well sampled in those compositions. On top of this condition, it is preferred to use compositions which thoroughly sample all interactions, i.e., compositions with "high entropy". To further sample frames/compositions for the energy, uncertainty quantification could again be used,[56] or the local predicted rigidity of compositions could be quantified.[60]

Here, we studied a 3-component system, but we had the constraint that the number of anions remained the same (to enforce electroneutrality), which meant we only needed 2 unique compositions to ensure the energy is transferable, even though we could only learn the energies of each ion up to some constant. If, for example, we had two ILs with different cations and anions that could be mixed together, we would again only need 2 compositions as we have 2 constraints of the electroneutrality of each salt, which means we can determine the energy of each salt, but not necessarily the ions within each salt. Again, sampling compositions near 0.5, the high entropy state, will allow interactions between ions to be well sampled. Consider again a case of a system with 2 types of cations and 2 types of anions, but there are 4 salts from the mixtures of cations−anions that we have access to. Even though we still require electroneutrality, we would require 4 compositions to determine the energy of each ion, as there are multiple ways of satisfying electroneutrality. This case should allow the energy of each ion to be determined without a constant and should allow the MLIP to be even more transferable. This logic can be extended to other complex mixtures, not just electrolytes, and the results are expected to be robust and useful for anyone training bespoke models of complex mixtures using these methods.

These results are not the first time transferable MLIPs have been investigated, but as far as the authors are aware, it is the first time some general guidelines have been clearly outlined. In ref 59 Yoo et al. noted that when developing a transferable model for mixtures of Ge−Te, training on a single mixture near a 1:1 ratio was not accurate, but when training on all the compositions studied (5 in total), satisfactory generalization was obtained. From the guidelines outlined here, we expect that only 2 compositions would be needed. In ref 61, Chahal et al. investigated a molten salt mixture, LiF−NaF−ZrF_4. They also found that training on a single composition did not produce adequate transferability and reported training on 42−29−29 and 26−37−37 mol % resulted in a satisfactory model.

https://doi.org/10.1021/acs.jpclett.4c01942
J. Phys. Chem. Lett. 2024, 15, 7539−7547

This model was tested on 38−51−11, 40−46−14, and 28−32−40, and it was demonstrated that their model could capture various properties, such as coordination numbers and diffusion coefficients. We expect their developed model has learnt forces to be transferable, owing to "high-entropy" mixtures being trained on, but as LiF−NaF−ZrF_4 could be considered as a 3-component salt mixture, we expect 3 compositions would be needed to learn the energy to be generalizable for different salt ratios. It is expected, however, that their model has learned how the energy changes when changing the ratio of LiF to NaF−ZrF_4, owing to different LiF to NaF−ZrF_4 being sampled. As compositions relatively close to those trained on were tested, the energy errors incurred from generalization would not be serious and should not significantly alter their predictions for coordination numbers or diffusion coefficients, for example.

There has recently been significant efforts to develop "general" or "foundational" MLIPs[28,55,62−66] trained on large data sets, such as the Materials Project[67] or the SPICE data set.[68] We hope the quantitative approach taken here can be further developed and applied to these larger models to reveal their limitations and guide improvements. In the context of electrolytes, Gong et al.[69] have developed a large data set, for carbonate-based Li-ion electrolytes, and shown some initial results for chemical transferability, but further tests should be performed on this data set with the guidelines outlined here to understand the limitations of this data set.

As we have demonstrated that we can train a NequIP/Allegro model to be transferable, and some simple guidelines for how this can be achieved, we next move onto assessing the accuracy of Allegro when being applied to a novel system.

As summarized previously, many ILs are excellent "green solvents" for reactions.[1−3] One property in this area that requires extremely accurate energy predictions is the solubility of solutes, as any error in the energy change becomes exponentially worse for the solubility prediction.[8,70,71] For example, calculating the solubility of O_2 or CO_2 in ILs requires that these species are inserted into the IL and the energy change be calculated. Classical force fields have typically been used to compute solubilities, but the energy of insertion of these molecular species is not at the same level of accuracy as DFT, which means the solubility computed from classical force fields is sometimes erroneous.[70−72] MLIPs promise a way to bridge this gap: they are DFT-accurate but are still computationally cheap enough to perform such calculations.[73,74]

To work toward this goal, we synthesize and characterize (details in Supporting Information Section 1) a novel IL $[F\text{-}OMIM]^+[C_4F_9CO_2]^-$, the structure of which is shown in Figure 2a; that is of interest for its O_2 solubility.[8,36] As can be seen in Figure 2b, this IL has a highly heterogeneous, lamellar-like structure, which creates voids for O_2 to dissolve into.[8] In ref 8, the solubility of O_2 was correlated to thermal expansion and isothermal compressibility of the ILs, both of which are related to the formation of voids in the IL.[8] Therefore, we compare the experimental density, thermal expansion, and isothermal compressibility against the MLIP we develop for this novel IL.

We developed and tested the accuracy of an Allegro model for $[F\text{-}OMIM]^+[C_4F_9CO_2]^-$, while only using a small amount of data and only performing 1 iterative training round at most, as it is expensive to keep (re)training deep learning models. While developing this model, we investigated the role of how the data set was generated, and hyperparameter optimization for the errors and stability of the model, full details of which can be found in the Supporting Information Sections 4 and 5. Here we show results for only one model. Specifically a model with r_{max} = 7, l_{max} = 2, and n_{layers} = 2 (termed 722), which proved to be reliable, with a scale factor of 100 on the stress loss (termed 11100, as the scale of the energy and force are 1). Overall, we found using large r_{max} was required for accurate predictions of the density, which is perhaps not surprising, as large r_{max} captures more long-ranged electrostatics and dispersion interactions, and that l_{max} = 2 was essential for a chemically stable model. We also found using the data set of 180 frames generated from running short AIMD simulations, starting from the uncorrelated OPLS structures (see Supporting Information Sections 4 and 5), performed significantly better than training directly on the OPLS structures. Performing the short AIMD runs (only 50 steps) from the OPLS structures did not dramatically alter the structures but did lower the energy by ∼10 eV (with 530 atoms) and significantly reduced the pressure of the box, which suggests the quality of the data to be extremely important when in this light data regime. In addition, we included 40 frames of volume scans generated from a previous Allegro model. We validate the predictions of this model against DFT and our experiments.

To test this Allegro model, we run several short 100 ps NPT simulations with 530 atoms to collect 20 structure predictions (separated by ∼10 ps) and their corresponding energy and forces. In Figure 2c we show a parity plot for the forces predicted by Allegro in comparison to the DFT forces computed from these structures. Overall, excellent agreement can be found with force MAEs in the range 20−70 meV $Å^{-1}$. These errors are practically identical with the MAEs obtained validating the potential. Therefore, the Allegro model for $[F\text{-}OMIM]^+[C_4F_9CO_2]^-$ appears to have *ab initio* accurate forces for this IL, with only a small amount of DFT data. In Figure 2d we show how the energy evolves with the simulation from Allegro, and the frames are picked out to test the energy and forces on. In Figure 2d, we also show the corresponding DFT energy calculated from those structures. Clearly, the DFT energy is higher than the Allegro model for all tested structures, by ∼2−4 meV/atom, which is several times the error obtained from the data set that it is tested on, albeit still a respectable value for the amount of data. Importantly, the difference in energy does not get significantly worse with time. In Figure 2e we further show this with an energy parity plot, where the DFT values are clearly larger than the Allegro energies. It is likely that this difference between Allegro and DFT originates from long-ranged interactions, as Allegro is a strictly local model.[27] Further development of these methods to include long-ranged interactions should improve the accuracy of the models.[15,76,77]

In Figure 2f we show the density predictions of our Allegro model for $[F\text{-}OMIM]^+[C_4F_9CO_2]^-$ at various temperatures, calculated from the last half of a 1 ns NPT run with 4240 atoms at 1 bar, and we also show the predictions from the classical force field and the experimental values. The experiment finds the density of $[F\text{-}OMIM]^+[C_4F_9CO_2]^-$ to be slightly less than 1.7 g cm^{-3} at 300 K, decreasing with temperature to 1.64 g cm^{-3} at 340 K. The values from the classical force field are extremely close to the experimental values because the charges were rescaled such that the density matched the experimental density (see Supporting Information Section 4). The density prediction from the Allegro model for

https://doi.org/10.1021/acs.jpclett.4c01942
J. Phys. Chem. Lett. 2024, 15, 7539−7547

$[F\text{-}OMIM]^+[C_4F_9CO_2]^-$ is 1.61 g cm^{-3} at 300 K. The difference between the Allegro model and experiments could be attributed to the employed PBE exchange-correlation functional, as found by others.[23,25] Despite this, the thermal expansion from Allegro, -1.03×10^{-3} g cm^{-3} K^{-1}, agrees reasonably well with that from experiments, -1.32×10^{-3} g cm^{-3} K^{-1}. Moreover, the isothermal compressibility of $[F\text{-}OMIM]^+[C_4F_9CO_2]^-$ is determined to be 8.6×10^{-10} Pa^{-1} at 298 K from experiments, and from fitting the Tait equation of state to the results from our Allegro model, we find a value of 6.46×10^{-10} Pa^{-1} at 300 K. While the thermal expansion and isothermal compression are not in perfect agreement with experiments, they are within what can be expected from the employed exchange-correlation functional, as others have found for different ILs and molten salts,[23,25] which appears to be the main limitation.

Overall, we have demonstrated that the equivariant MLIPs, NequIP and Allegro, can be used for data-efficient, transferable, and accurate simulations of ILs and their mixtures. Specifically, we first showed that there exists a minimum number of compositions that need to be trained on to learn the energy to be transferable using a salt-doped IL as the test case. In contrast, forces could be learned to be transferable with any number of compositions, but sampling "high-entropy" compositions often worked better than sampling pure compositions. Second, we demonstrated that these methods could be used for accurate simulations of a novel IL. Moreover, we showed that only ∼200 DFT frames with 1 iterative training loop were needed for reasonable robustness, demonstrating the data-efficient nature of the method. We did, however, find that how the data were generated was important, with frames generated from short AIMD runs being more reliable than frames generated from classical force fields. The main limitation of the method is the employed DFT settings, but now a method to accurately train them has been outlined; more accurate and expensive methods can be employed.

■ ASSOCIATED CONTENT

Supporting Information

The Supporting Information is available free of charge at https://pubs.acs.org/doi/10.1021/acs.jpclett.4c01942.

Experimental synthesis and characterization; additional simulation methods and results (PDF)

■ AUTHOR INFORMATION

Corresponding Authors

Zachary A. H. Goodwin − *John A. Paulson School of Engineering and Applied Sciences, Harvard University, Cambridge, Massachusetts 02138, United States;* orcid.org/0000-0003-2760-4499; Email: zgoodwin@seas.harvard.edu

Boris Kozinsky − *John A. Paulson School of Engineering and Applied Sciences, Harvard University, Cambridge, Massachusetts 02138, United States; Research and Technology Center, Robert Bosch LLC, Cambridge, Massachusetts 02142, United States;* orcid.org/0000-0002-0638-539X; Email: bkoz@seas.harvard.edu

Nicola Molinari − *John A. Paulson School of Engineering and Applied Sciences, Harvard University, Cambridge, Massachusetts 02138, United States; Research and Technology Center, Robert Bosch LLC, Cambridge, Massachusetts 02142, United States;* orcid.org/0000-0002-2913-7030; Email: nmolinari@seas.harvard.edu

Authors

Malia B. Wenny − *Department of Chemistry and Chemical Biology, Harvard University, Cambridge, Massachusetts 02138, United States;* orcid.org/0000-0002-0704-8184

Julia H. Yang − *John A. Paulson School of Engineering and Applied Sciences, Harvard University, Cambridge, Massachusetts 02138, United States; Harvard University Center for the Environment, Cambridge, Massachusetts 02138, United States;* orcid.org/0000-0002-5713-2288

Andrea Cepellotti − *John A. Paulson School of Engineering and Applied Sciences, Harvard University, Cambridge, Massachusetts 02138, United States*

Jingxuan Ding − *John A. Paulson School of Engineering and Applied Sciences, Harvard University, Cambridge, Massachusetts 02138, United States*

Kyle Bystrom − *John A. Paulson School of Engineering and Applied Sciences, Harvard University, Cambridge, Massachusetts 02138, United States;* orcid.org/0000-0003-1342-4972

Blake R. Duschatko − *John A. Paulson School of Engineering and Applied Sciences, Harvard University, Cambridge, Massachusetts 02138, United States*

Anders Johansson − *John A. Paulson School of Engineering and Applied Sciences, Harvard University, Cambridge, Massachusetts 02138, United States*

Lixin Sun − *John A. Paulson School of Engineering and Applied Sciences, Harvard University, Cambridge, Massachusetts 02138, United States;* orcid.org/0000-0002-7971-5222

Simon Batzner − *John A. Paulson School of Engineering and Applied Sciences, Harvard University, Cambridge, Massachusetts 02138, United States*

Albert Musaelian − *John A. Paulson School of Engineering and Applied Sciences, Harvard University, Cambridge, Massachusetts 02138, United States*

Jarad A. Mason − *Department of Chemistry and Chemical Biology, Harvard University, Cambridge, Massachusetts 02138, United States;* orcid.org/0000-0003-0328-7775

Complete contact information is available at: https://pubs.acs.org/10.1021/acs.jpclett.4c01942

Notes

The authors declare no competing financial interest.

■ ACKNOWLEDGMENTS

We thank Rajni Chahal and Stephen Lam for discussions and confirming our predictions of the energy generalization of their work is accurate. This work used beamline 12-ID-B at the Advanced Photon Source, a U.S. Department of Energy (DOE) Office of Science User Facility operated for the DOE Office of Science by Argonne National Laboratory under Contract DE-AC02-06CH11357. This research was supported under a Multidisciplinary University Research Initiative, sponsored by the Department of the Navy, Office of Naval Research, under Grant N00014-20-1-2418. Work at Harvard by Z.A.H.G., J.H.Y., A.C., J.D., K.B., B.R.D, A.J., L.S., S.B., A.M., B.K., and N.M. was supported by Robert Bosch Research North America. J.H.Y. acknowledges funding from the Harvard University Center for the Environment. J.A.M. acknowledges support from the Arnold and Mabel Beckman Foundation

through a Beckman Young Investigator grant. B.R.D. was supported by a NASA Space Technology Graduate Research Opportunity, under Grant 80NSSC20K1189. A.J. was supported by an Aker Scholarship.

REFERENCES

(1) Welton, T. Room-temperature ionic liquids: solvents for synthesis and catalysis. *Chem. Rev.* **1999**, *99*, 2071−2084.
(2) Weingärtner, H. Understanding ionic liquids at the molecular level: facts, problems, and controversies. *Angew. Chem., Int. Ed.* **2008**, *47*, 654−670.
(3) Hallett, J. P.; Welton, T. Room-temperature ionic liquids: solvents for synthesis and catalysis. 2. *Chem. Rev.* **2011**, *111*, 3508−3576.
(4) Fedorov, M. V.; Kornyshev, A. A. Ionic liquids at electrified interfaces. *Chem. Rev.* **2014**, *114*, 2978−3036.
(5) Watanabe, M.; Thomas, M. L.; Zhang, S.; Ueno, K.; Yasuda, T.; Dokko, K. Application of ionic liquids to energy storage and conversion materials and devices. *Chem. Rev.* **2017**, *117*, 7190−7239.
(6) Yao, N.; Chen, X.; Fu, Z.-H.; Zhang, Q. Applying classical, ab initio, and machine-learning molecular dynamics simulations to the liquid electrolyte for rechargeable batteries. *Chem. Rev.* **2022**, *122*, 10970−11021.
(7) Hu, Y.-F.; Liu, Z.-C.; Xu, C.-M.; Zhang, X.-M. The molecular characteristics dominating the solubility of gases in ionic liquids. *Chem. Soc. Rev.* **2011**, *40*, 3802−3823.
(8) Wenny, M. B.; Molinari, N.; Slavney, A. H.; Thapa, S.; Lee, B.; Kozinsky, B.; Mason, J. A. Understanding relationships between free volume and oxygen absorption in ionic liquids. *J. Phys. Chem. B* **2022**, *126*, 1268−1274.
(9) Niedermeyer, H.; Hallett, J. P.; Villar-Garcia, I. J.; Hunt, P. A.; Welton, T. Mixtures of ionic liquids. *Chem. Soc. Rev.* **2012**, *41*, 7780−7802.
(10) Izgorodina, E. I.; Seeger, Z. L.; Scarborough, D. L. A.; Tan, S. Y. S. Quantum chemical methods for the prediction of energetic, physical, and spectroscopic properties of ionic liquids. *Chem. Rev.* **2017**, *117*, 6696−6754.
(11) Dong, K.; Liu, X.; Dong, H.; Zhang, X.; Zhang, S. Multiscale studies on ionic liquids. *Chem. Rev.* **2017**, *117*, 6636−6695.
(12) Jeanmairet, G.; Rotenberg, B.; Salanne, M. Microscopic simulations of electrochemical double-layer capacitors. *Chem. Rev.* **2022**, *122*, 10860−10898.
(13) McEldrew, M.; Goodwin, Z. A. H.; Zhao, H.; Bazant, M. Z.; Kornyshev, A. A. Correlated ion transport and the gel phase in room temperature ionic liquids. *J. Phys. Chem. B* **2021**, *125*, 2677−2689.
(14) Dajnowicz, S.; Agarwal, G.; Stevenson, J. M.; Jacobson, L. D.; Ramezanghorbani, F.; Leswing, K.; Friesner, R. A.; Halls, M. D.; Abel, R. High-dimensional neural network potential for liquid electrolyte simulations. *J. Phys. Chem. B* **2022**, *126*, 6271−6280.
(15) Behler, J. Four generations of high-dimensional neural network potentials. *Chem. Rev.* **2021**, *121*, 10037−10072.
(16) Deringer, V. L.; Caro, M. A.; Csányi, G. Machine learning interatomic potentials as emerging tools for materials science. *Adv. Mater.* **2019**, *31*, 1902765.
(17) Unke, O. T.; Chmiela, S.; Sauceda, H. E.; Gastegger, M.; Poltavsky, I.; Schütt, K. T.; Tkatchenko, A.; Müller, K.-R. Machine learning force fields. *Chem. Rev.* **2021**, *121*, 10142−10186.
(18) Deringer, V. L.; Bartók, A. P.; Bernstein, N.; Wilkins, D. M.; Ceriotti, M.; Csányi, G. Gaussian process regression for materials and molecules. *Chem. Rev.* **2021**, *121*, 10073−10141.
(19) Batzner, S.; Musaelian, A.; Kozinsky, B. Advancing molecular simulation with equivariant interatomic potentials. *Nat. Rev. Phys.* **2023**, *5*, 437−438.
(20) Montes-Campos, H.; Carrete, J.; Bichelmaier, S.; Varela, L. M.; Madsen, G. K. H. A differentiable neural-network force field for ionic liquids. *J. Chem. Inf. Model.* **2022**, *62*, 88−101.
(21) Ling, Y.; Li, K.; Wang, M.; Lu, J.; Wang, C.; Wang, Y.; He, H. Revisiting the structure, interaction, and dynamical property of ionic liquid from the deep learning force field. *J. Power Sources* **2023**, *555*, 232350.
(22) Tovey, S.; Krishnamoorthy, A. N.; Sivaraman, G.; Guo, J.; Benmore, C.; Heuer, A.; Holm, C. DFT accurate interatomic potential for molten NaCl from machine learning. *J. Phys. Chem. C* **2020**, *124*, 25760−25768.
(23) Li, Q.-J.; Küçükbenli, E.; Lam, S.; Khaykovich, B.; Kaxiras, E.; Li, J. Development of robust neural-network interatomic potential for molten salt. *Cell Rep.* **2021**, *2*, 100359.
(24) Mondal, A.; Kussainova, D.; Yue, S.; Panagiotopoulos, A. Z. Modeling chemical reactions in alkali carbonate-hydroxide electrolytes with deep learning potentials. *J. Chem. Theory Comput.* **2023**, *19*, 4584−4595.
(25) Liang, W.; Lu, G.; Yu, J. Molecular dynamics simulations of molten magnesium chloride using machine-learning-based deep potential. *Adv. Theory Simul.* **2020**, *3*, 2000180.
(26) Batzner, S.; Musaelian, A.; Sun, L.; Geiger, M.; Mailoa, J. P.; Kornbluth, M.; Molinari, N.; Smidt, T. E.; Kozinsky, B. E(3)-equivariant graph neural networks for data-efficient and accurate interatomic potentials. *Nat. Commun.* **2022**, *13*, 2453.
(27) Musaelian, A.; Batzner, S.; Johansson, A.; Sun, L.; Owen, C. J.; Kornbluth, M.; Kozinsky, B. Learning local equivariant representations for large-scale atomistic dynamics. *Nat. Commun.* **2023**, *14*, 579.
(28) Musaelian, A.; Johansson, A.; Batzner, S.; Kozinsky, B. *Scaling the leading accuracy of deep equivariant models to biomolecular simulations of realistic size*. arXiv:2304.10061 (accessed 2024-02-18), 2023.
(29) Batatia, I.; Kovács, D. P.; Simm, G. N. C.; Ortner, C.; Csányi, G. *MACE: higher order equivariant message passing neural networks for fast and accurate force fields*. arXiv:2206.07697 (accessed 2024-02-04), 2022.
(30) Molinari, N.; Mailoa, J. P.; Kozinsky, B. General trend of a negative Li effective charge in ionic liquid electrolytes. *J. Phys. Chem. Lett.* **2019**, *10*, 2313−2319.
(31) Molinari, N.; Mailoa, J. P.; Craig, N.; Christensen, J.; Kozinsky, B. Transport anomalies emerging from strong correlation in ionic liquid electrolytes. *J. Power Sources* **2019**, *428*, 27−36.
(32) McEldrew, M.; Goodwin, Z. A. H.; Molinari, N.; Kozinsky, B.; Kornyshev, A. A.; Bazant, M. Z. Salt-in-ionic-liquid electrolytes: Ion network formation and negative effective charges of alkali metal cations. *J. Phys. Chem. B* **2021**, *125*, 13752−13766.
(33) Goodwin, Z. A.; McEldrew, M.; Kozinsky, B.; Bazant, M. Z. Theory of cation solvation and ionic association in nonaqueous solvent mixtures. *PRX Energy* **2023**, *2*, 013007.
(34) Gouverneur, M.; Schmidt, F.; Schönhoff, M. Negative effective Li transference numbers in Li salt/ionic liquid mixtures: does Li drift in the "wrong" direction? *Phys. Chem. Chem. Phys.* **2018**, *20*, 7470−7478.
(35) Brinkkötter, M.; Mariani, A.; Jeong, S.; Passerini, S.; Schönhoff, M. Ionic liquid in Li salt electrolyte: modifying the Li^+ transport mechanism by coordination to an asymmetric anion. *Adv. Energy Sustainability Res.* **2021**, *2*, 2000078.
(36) Wenny, M. B.; Walter, M. V.; Slavney, A. H.; Mason, J. A. Generalizable synthesis of highly fluorinated ionic liquids. *J. Phys. Chem. B* **2023**, *127*, 2028−2033.
(37) Fadel, E. R.; Faglioni, F.; Samsonidze, G.; Molinari, N.; Merinov, B. V.; Goddard, W. A., III; Grossman, J. C.; Mailoa, J. P.; Kozinsky, B. Role of solvent-anion charge transfer in oxidative degradation of battery electrolytes. *Nat. Commun.* **2019**, *10*, 1−10.
(38) Molinari, N.; Kozinsky, B. Chelation-induced reversal of negative cation transference number in ionic liquid electrolytes. *J. Phys. Chem. B* **2020**, *124*, 2676−2684.
(39) Molinari, N.; Khawaja, M.; Sutton, A.; Mostofi, A. Molecular model for HNBR with tunable cross-link density. *J. Phys. Chem. B* **2016**, *120*, 12700−12707.
(40) Hoover, W. G. Canonical dynamics: equilibrium phase-space distributions. *Phys. Rev. A* **1985**, *31*, 1695.
(41) Nosé, S. A unified formulation of the constant temperature molecular dynamics methods. *J. Chem. Phys.* **1984**, *81*, 511−519.

https://doi.org/10.1021/acs.jpclett.4c01942
J. Phys. Chem. Lett. 2024, 15, 7539−7547

(42) Hoover, W. G. Constant-pressure equations of motion. *Phys. Rev. A* **1986**, *34*, 2499.
(43) Plimpton, S. Fast Parallel Algorithms for Short-range Molecular Dynamics. *J. Comput. Phys.* **1995**, *117*, 1−19.
(44) Thompson, A. P.; Aktulga, H. M.; Berger, R.; Bolintineanu, D. S.; Brown, W. M.; Crozier, P. S.; in 't Veld, P. J.; Kohlmeyer, A.; Moore, S. G.; Nguyen, T. D.; et al. LAMMPS - a flexible simulation tool for particle-based materials modeling at the atomic, meso, and continuum scales. *Comput. Phys. Commun.* **2022**, *271*, 10817.
(45) Jorgensen, W. L.; Tirado-Rives, J. The OPLS [optimized potentials for liquid simulations] potential functions for proteins, energy minimizations for crystals of cyclic peptides and crambin. *J. Am. Chem. Soc.* **1988**, *110*, 1657−1666.
(46) Doherty, B.; Zhong, X.; Gathiaka, S.; Li, B.; Acevedo, O. Revisiting OPLS force field parameters for ionic liquid simulations. *J. Chem. Theory Comput.* **2017**, *13*, 6131−6145.
(47) Mogurampelly, S.; Ganesan, V. Structure and mechanisms underlying ion transport in ternary polymer electrolytes containing ionic liquids. *J. Chem. Phys.* **2017**, *146*, 074902.
(48) Pal, T.; Beck, C.; Lessnich, D.; Vogel, M. Effects of silica surfaces on the structure and dynamics of room-temperature ionic liquids: a molecular dynamics simulation study. *J. Phys. Chem. C* **2018**, *122*, 624−634.
(49) Giannozzi, P.; Baroni, S.; Bonini, N.; Calandra, M.; Car, R.; Cavazzoni, C.; Ceresoli, D.; Chiarotti, G. L.; Cococcioni, M.; Dabo, I.; et al. QUANTUM ESPRESSO: a modular and open-source software project for quantum simulations of materials. *J. Phys.: Condens. Matter* **2009**, *21*, 395502.
(50) Giannozzi, P.; Andreussi, O.; Brumme, T.; Bunau, O.; Nardelli, M. B.; Calandra, M.; Car, R.; Cavazzoni, C.; Ceresoli, D.; Cococcioni, M.; et al. Advanced capabilities for materials modelling with Quantum ESPRESSO. *J. Phys.: Condens. Matter* **2017**, *29*, 465901.
(51) Perdew, J. P.; Burke, K.; Ernzerhof, M. Generalized gradient approximation made simple. *Phys. Rev. Lett.* **1996**, *77*, 3865−3868.
(52) Grimme, S.; Antony, J.; Ehrlich, S.; Krieg, H. A consistent and accurate ab initio parametrization of density functional dispersion correction (DFT-D) for the 94 elements H-Pu. *J. Chem. Phys.* **2010**, *132*, 154104.
(53) Garrity, K. F.; Bennett, J. W.; Rabe, K. M.; Vanderbilt, D. Pseudopotentials for high-throughput DFT calculations. *Comput. Mater. Sci.* **2014**, *81*, 446−452.
(54) Zhang, L.; Han, J.; Wang, H.; Car, R.; E, W. Deep potential molecular dynamics: a scalable model with the accuracy of quantum mechanics. *Phys. Rev. Lett.* **2018**, *120*, 143001.
(55) Batatia, I.; Benner, P.; Chiang, Y.; Elena, A. M.; Kovács, D. P.; Riebesell, J.; Advincula, X. R.; Asta, M.; Avaylon, M.; Baldwin, W. J.; et al. *A foundation model for atomistic materials chemistry*. arXiv:2401.00096 (accessed 2024-01-12), 2023.
(56) Zhu, A.; Batzner, S.; Musaelian, A.; Kozinsky, B. Fast uncertainty estimates in deep learning interatomic potentials. *J. Chem. Phys.* **2023**, *158*, 164111.
(57) Vandermause, J.; Torrisi, S. B.; Batzner, S.; Xie, Y.; Sun, L.; Kolpak, A. M.; Kozinsky, B. On-the-fly active learning of interpretable Bayesian force fields for atomistic rare events. *npj Comput. Mater.* **2020**, *6*, 20.
(58) Xie, Y.; Vandermause, J.; Ramakers, S.; Protik, N. H.; Johansson, A.; Kozinsky, B. Uncertainty-aware molecular dynamics from bayesian active learning: phase transformations and thermal transport in SiC. *npj Comput. Mater.* **2023**, *9*, 36.
(59) Yoo, D.; Lee, K.; Jeong, W.; Lee, D.; Watanabe, S.; Han, S. Atomic energy mapping of neural network potential. *Phys. Rev. Materials* **2019**, *3*, 093802.
(60) Chong, S.; Grasselli, F.; Mahmoud, C. B.; Morrow, J. D.; Deringer, V. L.; Ceriotti, M. Robustness of local predictions in atomistic machine learning models. *J. Chem. Theory Comput.* **2023**, *19*, 8020−8031.
(61) Chahal, R.; Roy, S.; Brehm, M.; Banerjee, S.; Bryantsev, V.; Lam, S. T. Transferable deep learning potential reveals intermediate-range ordering effects in LiF-NaF-ZrF_4 molten salt. *JACS Au* **2022**, *2*, 2693−2702.
(62) Chen, C.; Ong, S. P. A universal graph deep learning interatomic potential for the periodic table. *Nat. Comput. Sci.* **2022**, *2*, 718−728.
(63) Deng, B.; Zhong, P.; Jun, K.; Riebesell, J.; Han, K.; Bartel, C. J.; Ceder, G. Chgnet as a pretrained universal neural network potential for charge-informed atomistic modelling. *Nat. Mach. Intell.* **2023**, *5*, 1031−1041.
(64) Merchant, A.; Batzner, S.; Schoenholz, S. S.; Aykol, M.; Cheon, G.; Cubuk, E. D. Scaling deep learning for materials discovery. *Nature* **2023**, *624*, 80−85.
(65) Kovács, D. P.; Moore, J. H.; Browning, N. J.; Batatia, I.; Horton, J. T.; Kapil, V.; Witt, W. C.; Cole, I.-B. M. D. J.; Csányi, G. *MACE-OFF23: transferable machine learning force fields for organic molecules*. arXiv:2312.15211 (accessed 2014-01-12), 2023.
(66) Yang, H.; Hu, C.; Zhou, Y.; Liu, X.; Shi, Y.; Li, J.; Li, G.; Chen, Z.; Chen, S.; Zeni, C. et al. *MatterSim: a deep learning atomistic model across elements, temperatures and pressures*. arXiv:2405.04967 (2024-06-22), 2024.
(67) Jain, A.; Ong, S. P.; Hautier, G.; Chen, W.; Richards, W. D.; Dacek, S.; Cholia, S.; Gunter, D.; Skinner, D.; Ceder, G.; Persson, K. A. Commentary: The materials project: a materials genome approach to accelerating materials innovation. *APL Mater.* **2013**, *1*, 011002.
(68) Eastman, P.; Behara, P. K.; Dotson, D. L.; Galvelis, R.; Herr, J. E.; Horton, J. T.; Mao, Y.; Chodera, J. D.; Pritchard, B. P.; Wang, Y.; De Fabritiis, G.; Markland, T. E. SPICE, a dataset of drug-like molecules and peptides for training machine learning potentials. *Scientific Data* **2023**, *10*, 11.
(69) Gong, S.; Zhang, Y.; Mu, Z.; Pu, Z.; Wang, H.; Yu, Z.; Chen, M.; Zheng, T.; Wang, Z.; Chen, L. et al. *BAMBOO: a predictive and transferable machine learning force field framework for liquid electrolyte development*. arXiv:2404.07181 (accessed 2024-06-22), 2024.
(70) Liu, H.; Dai, S.; Jiang, D. Solubility of gases in a common ionic liquid from molecular dynamics based free energy calculations. *J. Phys. Chem. B* **2014**, *118*, 2719−2725.
(71) Khawaja, M.; Sutton, A. P.; Mostofi, A. A. Molecular simulation of gas solubility in nitrile nutadiene rubber. *J. Phys. Chem. B* **2017**, *121*, 287−297.
(72) Shi, W.; Thompson, R. L.; Albenze, E.; Steckel, J. A.; Nulwala, H. B.; Luebke, D. R. Contribution of the acetate anion to CO_2 solubility in ionic liquids: theoretical method development and experimental study. *J. Phys. Chem. B* **2014**, *118*, 7383−7394.
(73) Fukushima, S.; Ushijima, E.; Kumazoe, H.; Koura, A.; Shimojo, F.; Shimamura, K.; Misawa, M.; Kalia, R. K.; Nakano, A.; Vashishta, P. Thermodynamic integration by neural network potentials based on first-principles dynamic calculations. *Phys. Rev. B* **2019**, *100*, 214108.
(74) Jinnouchi, R.; Karsai, F.; Kresse, G. Making free-energy calculations routine: Combining first principles with machine learning. *Phys. Rev. B* **2020**, *101*, 060201.
(75) Stukowski, A. Visualization and analysis of atomistic simulation data with OVITO-the Open Visualization Tool. *Modelling Simul. Mater. Sci. Eng.* **2010**, *18*, 015012.
(76) Yue, S.; Muniz, M. C.; Andrade, M. F. C.; Zhang, L.; Car, R.; Panagiotopoulos, A. Z. When do short-range atomistic machinelearning models fall short? *J. Chem. Phys.* **2021**, *154*, 034111.
(77) Zhang, L.; Wang, H.; Muniz, M. C.; Panagiotopoulos, A. Z.; Car, R.; E, W. A deep potential model with long-range electrostatic interactions. *J. Chem. Phys.* **2022**, *156*, 124107.

https://doi.org/10.1021/acs.jpclett.4c01942
J. Phys. Chem. Lett. 2024, 15, 7539−7547